

Communication

Effect of a Conical Cellulose Structure on Horseradish Peroxidase Biomacromolecules

Yuri D. Ivanov ^{1,2,*} , Vadim Y. Tatur ³, Ivan D. Shumov ¹ , Andrey F. Kozlov ¹, Anastasia A. Valueva ¹, Irina A. Ivanova ¹, Maria O. Ershova ¹, Nina D. Ivanova ^{3,4}, Igor N. Stepanov ³, Andrei A. Lukyanitsa ^{3,5} and Vadim S. Ziborov ^{1,2}

¹ Institute of Biomedical Chemistry, Pogodinskaya Str., 10 Build. 8, Moscow 119121, Russia

² Joint Institute for High Temperatures of the Russian Academy of Sciences, Moscow 125412, Russia

³ Foundation of Perspective Technologies and Novations, Moscow 115682, Russia

⁴ Moscow State Academy of Veterinary Medicine and Biotechnology Named after Skryabin, Moscow 109472, Russia

⁵ Faculty of Computational Mathematics and Cybernetics, Moscow State University, Moscow 119991, Russia

* Correspondence: yurii.ivanov.nata@gmail.com

Abstract: The effect of a dielectric conical structure on the adsorption properties of an enzyme on mica was studied by atomic force microscopy (AFM) with the example of horseradish peroxidase (HRP). The cone used was a cellulose cone with a 60° apex angle. Namely, AFM allowed us to reveal an increase in the enzyme's aggregation during its adsorption onto mica from the solution incubated near the cone apex for 40 min—as compared with the control enzyme samples incubated far away from the cone. In contrast, no change in the HRP adsorption properties was observed after shorter (10 min) incubation of the sample near the cone. The enzymatic activity of HRP was found to be the same for all the enzyme samples studied. Our findings should be considered upon designing biosensors (in particular, those intended for highly sensitive diagnostic applications) and bioreactors containing conical structural elements. Furthermore, since HRP is widely employed as a model enzyme in studies of external impacts on enzymes determining food quality, our data can be of use in the development of food-processing methods based on the use of electromagnetic radiation (microwave treatment, radiofrequency heating, etc.).

Keywords: atomic force microscopy; horseradish peroxidase; cellulose; conical structure; electromagnetic field; protein aggregation; enzyme adsorption; biosensor



Citation: Ivanov, Y.D.; Tatur, V.Y.; Shumov, I.D.; Kozlov, A.F.; Valueva, A.A.; Ivanova, I.A.; Ershova, M.O.; Ivanova, N.D.; Stepanov, I.N.; Lukyanitsa, A.A.; et al. Effect of a Conical Cellulose Structure on Horseradish Peroxidase Biomacromolecules. *Appl. Sci.* **2022**, *12*, 11994. <https://doi.org/10.3390/app122311994>

Academic Editor: Ramona Iseppi

Received: 20 October 2022

Accepted: 22 November 2022

Published: 24 November 2022

Publisher's Note: MDPI stays neutral with regard to jurisdictional claims in published maps and institutional affiliations.



Copyright: © 2022 by the authors. Licensee MDPI, Basel, Switzerland. This article is an open access article distributed under the terms and conditions of the Creative Commons Attribution (CC BY) license (<https://creativecommons.org/licenses/by/4.0/>).

1. Introduction

The influence of electromagnetic and magnetic fields on biological systems is considered in numerous papers. This influence manifests itself not only at the macroscopic level (that is, at the level of the entire organism [1,2]), but also at the level of enzymes [2–9]. Electromagnetic fields of even relatively low power were demonstrated to affect the aggregation [9] and other properties of enzymes [5]. Data on the influence of geometric bodies of various shapes on enzyme systems in background electromagnetic fields are beginning to appear in the literature [10–13]. Namely, Balezin et al. [10] considered the calculations of changes in the spatial topography of an electromagnetic field in a pyramid, which was made of a dielectric material. These authors raised the question about the concentration of electromagnetic fields near pyramidal structures of both nanometer (and this is related to atomic force microscopy (AFM) probes) and much larger objects. Moreover, changes in the topography of background electromagnetic fields were reported to affect the physicochemical properties of enzymes incubated near pyramidal structures [9,13]. It was also demonstrated that incubation near spherical elements can also affect the properties of enzymes [12]. In this connection, the question is whether the structures of other shapes

(different from pyramidal and spherical ones) influence an enzyme's properties. It is necessary to address this problem, since it is associated with the development of enzyme-based biosensors. This issue is also important in designing specialized rooms for experiments with highly sensitive equipment. Namely, the use of conical shape elements in the construction of anechoic chambers, which are designed to suppress external electromagnetic interference when working with highly sensitive equipment [14], should be emphasized. Highly sensitive biosensors such as nanowire detectors [15–17] are just the case in this respect. The use of elements of conical shape in biosensors was also reported [18,19].

In our present work, the influence of a conical dielectric structure on an enzyme was studied by AFM. Owing to its ultra-high height resolution, this method allows one to reveal even subtle changes in the properties of biological objects (including enzymes) upon studying their surface [12,20] down to the level of single macromolecules [9,12,21]. For instance, AFM was successfully used to reveal the effect of weak electromagnetic fields on an enzyme [9]. A cellulose cone was used as a model of a dielectric structure. Cellulose, being the main component of wood, has unique advantages as a material for use in biosensors and energy sources, as was emphasized by Fraiwan and Choi [22]. Cellulose is an inexpensive, biodegradable and flexible material with a large surface area, thus representing an excellent solution for manufacturing biobatteries [22]. Although the use of disposable cellulose biosensors in disease detection, health monitoring and environmental pollutant detection has been reported, the ability to access an external energy source further enhances their diagnostic capabilities [23]. Moreover, cellulose is employed for electromagnetic shielding [24]. In this connection, it is important to emphasize that cellulose was reported to interact with alternating electromagnetic fields at both the colloidal [25,26] and macroscopic [25] level.

As regards food-processing applications, peroxidases are responsible for enzymatic browning, which directly affects food quality [6,7,27,28], and the effects of treatment with the use of microwave [6] and radiofrequency [7,28] radiation on these enzymes thus represent an actual phenomenon in modern food science. In our experiments, we used the horseradish peroxidase (HRP) model enzyme. This 40 to 44 kDa [29,30] enzyme glycoprotein with relatively high carbohydrate content [31–33] is comprehensively characterized [29–34]. This is why it represents a very convenient model in studying external impacts (such as microwave [6] and radiofrequency [7] electromagnetic radiation, or the action of gas plasma [27,35–37]) on peroxidase-mediated processes in food [6,7,27,35–37].

Herein, the effect of a conical cellulose structure on the HRP enzyme was studied at the nanoscale for the first time. In our experiments, samples of buffered HRP solution were incubated near the cellulose conical structure. After the 40 min incubation, the enzyme was adsorbed from these samples onto the surface of mica substrates, whereon they were subsequently visualized by AFM. We have demonstrated that the incubation of a solution of HRP near the apex of a cellulose conical structure for 40 min leads to a change in the enzyme aggregation state on mica. Since cellulose is known to interact with electromagnetic fields [24–26], the effect observed can well take place as a result of the interaction of a cellulose conical structure with the background electromagnetic field. In this respect, our study is just one step further towards the understanding of this interaction, its effects and its applications. Our findings reported herein should be considered in the development of biosensors intended for highly sensitive protein detection in order to correctly account for the changes in the properties of the studied biological macromolecules in the course of the measurements.

2. Materials and Methods

2.1. Chemicals and Protein

Peroxidase from horseradish (Cat. #6782) and its substrate 2,2'-azino-bis(3-ethylbenzothiazoline-6-sulfonate) (ABTS; Cat. #A1888) were purchased from Sigma (St. Louis, MO, USA). Disodium hydrogen orthophosphate (Na_2HPO_4), citric acid and hydrogen peroxide (H_2O_2) were all of analytical or higher-purity grade, and were purchased

from Reakhim (Moscow, Russia). Dulbecco's modified phosphate-buffered saline was prepared by dissolving a salt mixture, commercially available from Pierce (Waltham, MA, USA), in ultrapure water. All the solutions used in our experiments were prepared using deionized ultrapure water (with $18.2 \text{ M}\Omega \times \text{cm}$ resistivity), obtained with a Simplicity UV system (Millipore, Molsheim, France).

2.2. Experimental Setup

In the study, a setup schematically shown in Figure 1 was used. An Eppendorf-type test tube with 1 mL of a 10^{-7} M solution of horseradish peroxidase in 2 mM PBS buffer (pH = 7.4) was placed at a 2 cm distance from the apex of the cellulose cone. In the control experiments, the test tubes were placed far away from the setup (at a >10 m distance, but in the same room). The material of the cone was wood, and its geometry was as follows: the cone base diameter was 220 mm, and the apex angle was 60° —analogous to the geometry of conical elements used in anechoic chambers used for electromagnetic shielding [14].

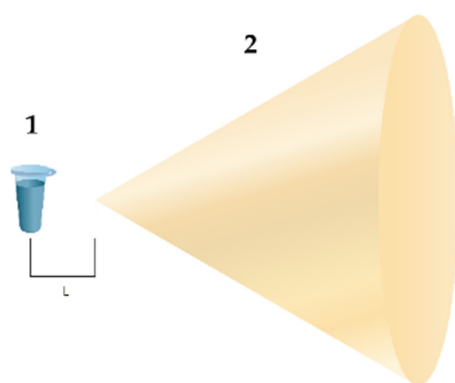


Figure 1. Experimental setup. Numbers indicate the main elements of the setup: (1) is the test tube with $0.1 \mu\text{M}$ HRP solution in 2 mM PBS buffer, and (2) is the cellulose cone. The distance between the test tube and the cone apex is $L = 2 \text{ cm}$.

The HRP solutions were incubated either in the vicinity or far away from the cone for either 10 or 40 min. To determine the physicochemical properties of HRP after the incubation, the solutions were subjected to AFM and spectrophotometric analysis with the use of well-established techniques reported in our previous papers [9,11–13].

2.3. Atomic Force Microscopy

In the course of the AFM experiments, the enzyme was captured onto the surface of mica substrates by direct surface adsorption [38] following the well-established technique described in our previous papers [9,11–13]. The relative density of the distribution of the imaged objects with height $\rho(h)$ was calculated as described by Pleshakova et al. [39]. The change in protein aggregation was analyzed as reported by Ivanov et al. [13]. Blank experiments were performed with the use of enzyme-free buffer instead of HRP solution, and we did not observe any objects with heights $> 0.5 \text{ nm}$ in the blank experiments.

2.4. Spectrophotometry

We estimated the HRP enzymatic activity using ABTS, following the technique described by Sanders et al. [40], in phosphate-citrate buffer [40,41] at pH 5.0 [40–42] as described in our previous papers [9,11–13].

3. Results

Figure 2 shows typical AFM images of the mica substrate surface with adsorbed HRP biomacromolecules adsorbed from their solutions incubated either far away (Figure 2a; control experiment) or near the apex of the cone (Figure 2b; working experiment) for 40 min.

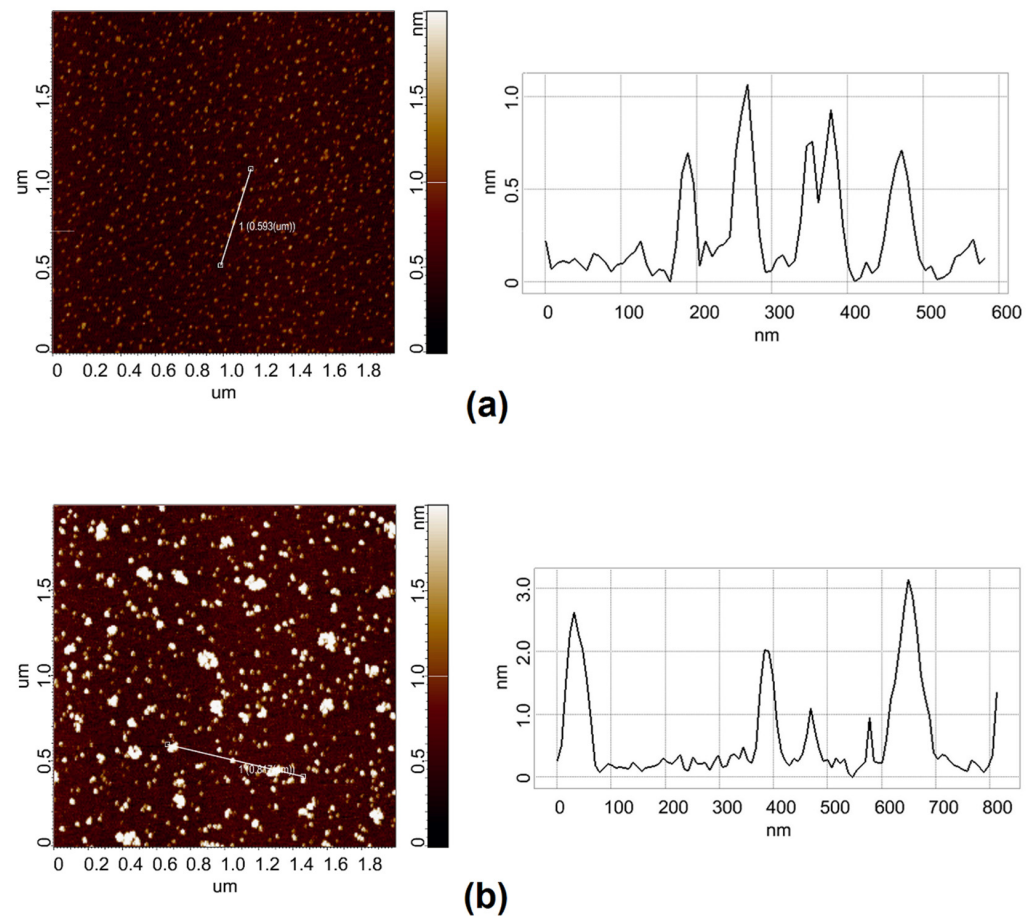


Figure 2. Typical AFM images (left) and cross-section profiles (right) of HRP biomacromolecules adsorbed onto mica. In the control experiment (a), the HRP sample was incubated at a >10 m distance from the cone. In the working experiment (b), the HRP sample was incubated at a 2 cm distance from the apex of the cone. The incubation time was 40 min. Scan size: 2 μm × 2 μm. Panels on the right show cross-section profiles corresponding to the lines in the images on the left.

The AFM images in Figure 2 clearly indicate the enlargement of HRP particles on mica after the 40 min incubation of the enzyme sample near the cone apex in comparison with the control sample. In both the control and working experiments, compact objects with heights of 1 to 2 nm were observed on the surface. They can be considered HRP biomolecules, since such objects were not observed in the blank experiments. Moreover, for the samples incubated near the cone apex for 40 min, higher (up to 3 nm, Figure 2b, right panel) objects were observed. Furthermore, many of the mica-adsorbed particles were much more extended laterally in comparison with the control sample. The latter can be attributed to HRP aggregates. In contrast, at a shorter incubation time (10 min), there was no difference between the AFM images obtained for the control sample and the sample incubated near the cone.

Figure 3 displays plots of the relative distribution of the AFM-imaged objects with the height $\rho(h)$ obtained for the samples incubated for 40 min (the distributions obtained for the shorter incubation time of 10 min did not differ from the control one and are therefore not shown).

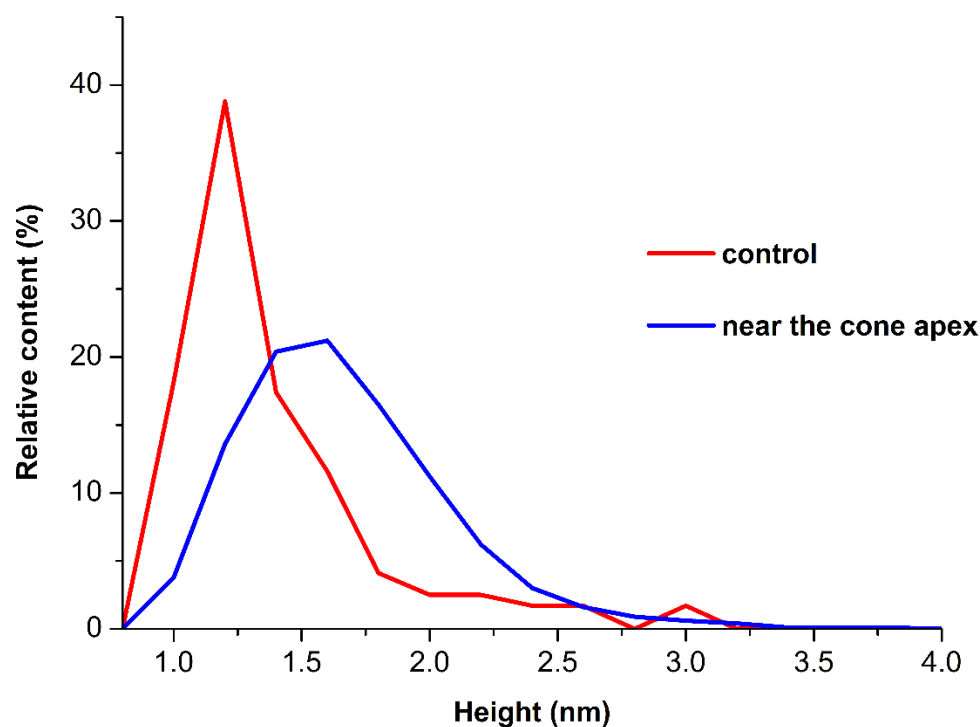


Figure 3. Plots of $\rho(h)$ distributions for the HRP samples incubated either near the cone apex (at $L = 2$ cm, working experiment; blue curve) or far away from the cone (at $L > 10$ m, control experiment; red curve).

As can be seen from Figure 3, in the working experiment, the maximum of the $\rho(h)$ distribution corresponded to $h_{max} = (1.6 \pm 0.2)$ nm, while in the control experiments, $h_{max} = (1.0 \pm 0.2)$ nm was obtained. Accordingly, the 40 min incubation near the cone apex led to a considerable shift in the distribution maximum to the right in comparison with the control experiments. However, the full width at half-maximum (FWHM) in the working experiments was 0.8 nm, while in the control experiments, a 0.4 nm FWHM was obtained. The molecular weight of HRP is 40 kDa [29,30]. The AFM images of monomeric biomolecules with approximately the same molecular weight have heights of 1–1.2 nm, depending on the experimental conditions [9]. Based on this, it can be claimed that the objects of ~1 nm height correspond to monomeric HRP, and it is this form of the enzyme that is adsorbed on the surface in both the working and the control experiments. However, in the working experiment, the distribution FWHM is much broader and, at the same time, the contribution of higher objects (which contribute to the right wing of the distribution, $h > 1.4$ nm) increases. The distribution width in the left wing indicates that the monomeric form of the enzyme, as well as aggregates of a higher degree of oligomerization (at which the height of objects increases), was observed. The increased contribution of objects to the right wing of the distribution in the working experiments indicates that the number of objects with a high degree of oligomerization increased in comparison with that for the control sample. The results of the AFM experiments indicate that the adsorption properties of HRP were affected after the incubation at a 2 cm distance from the cone apex for 40 min. Namely, such an incubation led to an increase in the degree of the aggregation of mica-adsorbed enzyme. After the incubation of the enzyme sample near the cone, the amount of aggregated HRP (including higher-order aggregates with $h > 1.8$ nm) increased considerably—as compared with the control sample incubated far away from the cone.

As regards the spectrophotometry measurements, the enzymatic activity of HRP was similar for all the samples studied.

4. Discussion

The results of our study indicate that the incubation of the HRP enzyme solution near the apex of the cellulose conical structure for 10 min does not affect the HRP's properties. In contrast, a longer incubation time (40 min) results in a change in the degree of the enzyme oligomerization on the mica surface. This indicates an effect of the incubation time on the properties of the enzyme. At the same time, no effect on the enzymatic activity of HRP is revealed.

The change in the degree of HRP oligomerization is likely to be caused by a change in the topology of the background electromagnetic field near the conical structure. Indeed, a theoretical investigation performed by Balezin et al. showed that a square pyramid can concentrate an electromagnetic field in the area of the pyramid's base [10]. A cone, in turn, also pertains to pyramid-like figures [43]. Namely, a cone represents a pyramid with a circular base [43]. The latter can be considered a polygon with an infinite number of sides [44]. Accordingly, the cone is also expected to interact with the background electromagnetic field, thus altering its topography, since such an effect has been observed for a square pyramid [11,13]. It has been shown that electric and electromagnetic fields of even low intensity can substantially alter the ratio between ortho- and para-isomers of water [45–47]. Artmann et al. demonstrated that the hydration shell of a biological macromolecule predominantly contains para-H₂O [48]. In our experiments, the background electromagnetic field could well be concentrated by the cellulose cone, thus affecting the hydration of the enzyme globule by altering the ratio between ortho- and para-H₂O in this shell. Additionally, the adsorption properties of the enzyme were changed at the expense of altered enzyme hydration [49,50]. This is how we explain the effect observed in our experiments.

The adsorption of macromolecules from their solution onto a solid substrate is determined by the interaction between the substrate (in our case, mica) surface and the surface of a hydrated enzyme globule, as well as by the interaction of the enzyme macromolecules with adjacent macromolecules in the solution, and with the solvent molecules [51]. This is why a change in enzyme hydration leads to a change in its oligomeric state on mica. Accordingly, there is a change in the contribution of aggregates of various orders to the relative distribution of AFM-visualized objects.

The results of our work can be of use in the development of biosensors intended for highly sensitive analysis, since a change in the hydration of biomacromolecules can result in a change in the functional properties [49,50]. The results obtained should also be considered in direct measurements using biosensors with conical constructive elements in order to protect the highly sensitive biosensors from external electromagnetic interference by means of anechoic chambers with conical elements. Since HRP is widely used as a model enzyme in studies of external impacts on enzymes determining food quality, our data can also be useful in the development of food-processing methods.

5. Conclusions

An effect of a conical cellulose structure on the enzyme adsorption at the nanoscale was revealed by AFM. The 40 min incubation of a 0.1 μ M aqueous solution of HRP enzyme at a 2 cm distance from the cellulose cone was found to cause a considerable increase in the formation of higher-order enzyme aggregates on mica. This effect is explained by the interaction of the cellulose cone with the background electromagnetic field, which is concentrated by the cone and acts on the enzyme hydration shell, thus influencing the enzyme adsorption on mica. HRP is widely used as a model in studies concerning applications of electromagnetic radiation (including radiofrequency and microwave ones) for the treatment of food products on the enzymes determining food quality. Our findings can also find application in the development of food-processing methods. Our study is one step further towards the understanding of the interaction of electromagnetic radiation with cellulose, its effects and its applications, and should be taken into account in the development of

novel electromagnetic shielding materials. Our results should also be considered in the development of biosensors and bioreactors intended for working with enzymes.

Author Contributions: Conceptualization, Y.D.I. and V.Y.T.; data curation, I.D.S., A.A.V. and M.O.E.; formal analysis, N.D.I., I.N.S. and V.S.Z.; investigation, I.D.S., A.F.K., A.A.V., I.A.I., M.O.E., I.N.S. and V.S.Z.; methodology, Y.D.I. and V.Y.T.; project administration, Y.D.I.; resources, V.Y.T., I.N.S., A.A.L. and V.S.Z.; software, A.A.L.; supervision, Y.D.I.; validation, V.S.Z.; visualization, I.D.S. and A.A.V.; writing—original draft, Y.D.I. and I.D.S.; writing—review and editing, Y.D.I. All authors have read and agreed to the published version of the manuscript.

Funding: This work was financed by the Ministry of Science and Higher Education of the Russian Federation within the framework of state support for the creation and development of World-Class Research Centers “Digital biodesign and personalized healthcare” No. 075-15-2022-305.

Data Availability Statement: Correspondence and requests for materials should be addressed to Y.D.I.

Acknowledgments: The AFM measurements were performed by employing a Titanium multimode atomic force microscope, which pertains to “Avogadro” large-scale research facilities.

Conflicts of Interest: The authors declare no conflict of interest.

References

- Diab, K.A. The Impact of the Low Frequency of the Electromagnetic Field on Human. *Adv. Exp. Med. Biol. Cell Biol. Trans. Med.* **2019**, *7*, 135–149. [\[CrossRef\]](#)
- Warille, A.A.; Altun, G.; Elamin, A.A.; Kaplan, A.A.; Mohamed, H.; Yurt, K.K.; Elhaj, A.E. Skeptical approaches concerning the effect of exposure to electromagnetic fields on brain hormones and enzyme activities. *J. Microsc. Ultrastruct.* **2017**, *5*, 177–184. [\[CrossRef\]](#) [\[PubMed\]](#)
- Wasak, A.; Drozd, R.; Jankowiak, D.; Rakoczy, R. The influence of rotating magnetic field on bio-catalytic dye degradation using the horseradish peroxidase. *Biochem. Eng. J.* **2019**, *147*, 81–88. [\[CrossRef\]](#)
- Caliga, R.; Maniu, C.L.; Mihășan, M. ELF-EMF exposure decreases the peroxidase catalytic efficiency in vitro. *Open Life Sci.* **2016**, *11*, 71–77. [\[CrossRef\]](#)
- Sun, J.; Sun, F.; Xu, B.; Gu, N. The quasi-one-dimensional assembly of horseradish peroxidase molecules in presence of the alternating magnetic field. *Coll. Surf. A Physicochem. Eng. Aspects* **2010**, *360*, 94–98. [\[CrossRef\]](#)
- Lopes, L.C.; Barreto, M.T.; Gonçalves, K.M.; Alvarez, H.M.; Heredia, M.F.; de Souza, R.O.M.; Cordeiro, Y.; Dariva, C.; Fricks, A.T. Stability and structural changes of horseradish peroxidase: Microwave versus conventional heating treatment. *Enzym. Microb. Technol.* **2015**, *69*, 10–18. [\[CrossRef\]](#)
- Yao, Y.; Zhang, B.; Pang, H.; Wang, Y.; Fu, H.; Chen, X.; Wang, Y. The effect of radio frequency heating on the inactivation and structure of horseradish peroxidase. *Food Chem.* **2023**, *398*, 133875. [\[CrossRef\]](#)
- Fortune, J.A.; Wu, B.-I.; Klivanov, A.M. Radio Frequency Radiation Causes No Nonthermal Damage in Enzymes and Living Cells. *Biotechnol. Prog.* **2010**, *26*, 1772–1776. [\[CrossRef\]](#)
- Ivanov, Y.D.; Pleshakova, T.O.; Shumov, I.D.; Kozlov, A.F.; Ivanova, I.A.; Valueva, A.A.; Tatur, V.Y.; Smelov, M.V.; Ivanova, N.D.; Ziborov, V.S. AFM imaging of protein aggregation in studying the impact of knotted electromagnetic field on a peroxidase. *Sci. Rep.* **2020**, *10*, 9022. [\[CrossRef\]](#)
- Balezin, M.; Baryshnikova, K.V.; Kapitanova, P.; Evlyukhin, A.B. Electromagnetic properties of the Great Pyramid: First multipole resonances and energy concentration. *J. Appl. Phys.* **2018**, *124*, 034903. [\[CrossRef\]](#)
- Ivanov, Y.D.; Pleshakova, T.O.; Shumov, I.D.; Kozlov, A.F.; Ivanova, I.A.; Valueva, A.A.; Ershova, M.O.; Tatur, V.Y.; Stepanov, I.N.; Repnikov, V.V.; et al. AFM study of changes in properties of horseradish peroxidase after incubation of its solution near a pyramidal structure. *Sci. Rep.* **2021**, *11*, 9907. [\[CrossRef\]](#) [\[PubMed\]](#)
- Ivanov, Y.D.; Tatur, V.Y.; Pleshakova, T.O.; Shumov, I.D.; Kozlov, A.F.; Valueva, A.A.; Ivanova, I.A.; Ershova, M.O.; Ivanova, N.D.; Repnikov, V.V.; et al. Effect of Spherical Elements of Biosensors and Bioreactors on the Physicochemical Properties of a Peroxidase Protein. *Polymers* **2021**, *13*, 1601. [\[CrossRef\]](#) [\[PubMed\]](#)
- Ivanov, Y.D.; Tatur, V.Y.; Pleshakova, T.O.; Shumov, I.D.; Kozlov, A.F.; Valueva, A.A.; Ivanova, I.A.; Ershova, M.O.; Ivanova, N.D.; Stepanov, I.N.; et al. The Effect of Incubation near an Inversely Oriented Square Pyramidal Structure on Adsorption Properties of Horseradish Peroxidase. *Appl. Sci.* **2022**, *12*, 4042. [\[CrossRef\]](#)
- Nakonechny, V.S.; Prisyazhny, A.E.; Poberezhny, A.A. Electrodynamical modeling using microwave anechoic chambers. Methodology for the anechoic factor estimation. *Syst. Inf. Proc.* **2005**, *9*, 116–123.
- Patolsky, F.; Zheng, G.; Hayden, O.; Lakadamyali, M.; Zhuang, X.; Lieber, C.M. Electrical detection of single viruses. *Proc. Natl. Acad. Sci. USA* **2004**, *101*, 14017–14022. [\[CrossRef\]](#)
- Zheng, G.; Patolsky, F.; Cui, Y.; Wang, W.U.; Lieber, C.M. Multiplexed electrical detection of cancer markers with nanowire sensor arrays. *Nat. Biotechnol.* **2005**, *23*, 1294–1301. [\[CrossRef\]](#) [\[PubMed\]](#)

17. Hahm, J.I.; Lieber, C.M. Direct ultrasensitive electrical detection of DNA and DNA sequence variations using nanowire nanosensors. *Nano Lett.* **2004**, *4*, 51–54. [[CrossRef](#)]
18. Arjmand, M.; Saghafifar, H.; Alijanianzadeh, M.; Soltanolkotabi, M. A sensitive tapered-fiber optic biosensor for the label-free detection of organophosphate pesticides. *Sens. Actuator B Chem.* **2017**, *249*, 523–532. [[CrossRef](#)]
19. Zitzmann, F.D.; Schmidt, S.; Naumann, M.; Belder, D.; Jahnke, H.-G.; Robitzki, A.A. Multielectrode biosensor chip for spatial resolution screening of 3D cell models based on microcavity arrays. *Biosens. Bioelectr.* **2022**, *202*, 114010. [[CrossRef](#)]
20. Laskowski, D.; Strzelecki, J.; Pawlak, K.; Dahm, H.; Balter, A. Effect of ampicillin on adhesive properties of bacteria examined by atomic force microscopy. *Micron* **2018**, *112*, 84–90. [[CrossRef](#)]
21. Pleshakova, T.O.; Malsagova, K.A.; Kaysheva, A.L.; Kopylov, A.T.; Tatur, V.Y.; Ziborov, V.S.; Ivanov, Y.D. Highly sensitive protein detection by biospecific AFM-based fishing with pulsed electrical stimulation. *FEBS Open Bio.* **2017**, *7*, 1186–1195. [[CrossRef](#)]
22. Fraiwan, A.; Choi, S. Bacteria-powered battery on paper. *Phys. Chem.* **2014**, *16*, 26288–26293. [[CrossRef](#)]
23. Ratajczak, K.; Stobiecka, M. High-performance modified cellulose paper-based biosensors for medical diagnostics and early cancer screening: A concise review. *Carbohydr. Polym.* **2020**, *229*, 115463. [[CrossRef](#)]
24. Li, M.; Zhao, Y.; Zhang, M.; Jiang, S.; Farooq, A.; Li, L.; Liu, L.; Ge, A.; Liu, L. Recent Progress in the Application of Cellulose in Electromagnetic Interference Shielding Materials. *Macromol. Mater. Eng.* **2022**, *307*, 2100899. [[CrossRef](#)]
25. Bordel, D.; Putaux, J.-L.; Heux, L. Orientation of Native Cellulose in an Electric Field. *Langmuir* **2006**, *22*, 4899–4901. [[CrossRef](#)]
26. Gindl, W.; Emsenhuber, G.; Maier, G.; Keckes, J. Cellulose in Never-Dried Gel Oriented by an AC electric field. *Biomacromolecules* **2009**, *10*, 1315–1318. [[CrossRef](#)] [[PubMed](#)]
27. Pipliya, S.; Kumar, S.; Srivastav, P.P. Inactivation kinetics of polyphenol oxidase and peroxidase in pineapple juice by dielectric barrier discharge plasma technology. *Innov. Food Sci. Emerg. Technol.* **2022**, *80*, 103081. [[CrossRef](#)]
28. Yao, Y.; Sun, Y.; Cui, B.; Fu, H.; Chen, X.; Wang, Y. Radio frequency energy inactivates peroxidase in stem lettuce at different heating rates and associate changes in physiochemical properties and cell morphology. *Food Chem.* **2021**, *342*, 128360. [[CrossRef](#)]
29. Davies, P.F.; Rennke, H.G.; Cotran, R.S. Influence of molecular charge upon the endocytosis and intracellular fate of peroxidase activity in cultured arterial endothelium. *J. Cell Sci.* **1981**, *49*, 69–86. [[CrossRef](#)]
30. Yan, Q.; Tang, X.; Zhang, B.; Wang, C.; Deng, S.; Ma, X.; Wang, C.; Li, D.; Huang, S.; Dong, P. Biocatalytic oxidation of flavone analogues mediated by general biocatalysts: Horseradish peroxidase and laccase. *RSC Adv.* **2019**, *9*, 13325–13331. [[CrossRef](#)] [[PubMed](#)]
31. Huddy, S.M.; Hitzeroth, I.L.; Meyers, A.E.; Weber, B.; Rybicki, E.P. Transient Expression and Purification of Horseradish Peroxidase C in *Nicotiana benthamiana*. *Int. J. Mol. Sci.* **2018**, *19*, 115. [[CrossRef](#)]
32. Welinder, K.G. Amino Acid Sequence Studies of Horseradish Peroxidase. Amino and Carboxyl Termini, Cyanogen Bromide and Tryptic Fragments, the Complete Sequence, and Some Structural Characteristics of Horseradish Peroxidase C. *JBIC J. Biol. Inorg. Chem.* **1979**, *96*, 483–502. [[CrossRef](#)]
33. Tams, J.W.; Welinder, K.G. Mild chemical deglycosylation of horseradish peroxidase yields a fully active, homogeneous enzyme. *Anal. Biochem.* **1995**, *228*, 48–55. [[CrossRef](#)]
34. Gajhede, M.; Schuller, D.J.; Henriksen, A.; Smith, A.T.; Poulos, T.L. Crystal structure of horseradish peroxidase C at 2.15 Å resolution. *Nat. Struct. Mol. Biol.* **1997**, *4*, 1032–1038. [[CrossRef](#)] [[PubMed](#)]
35. Dong, S.; Ma, Y.; Li, Y.; Xiang, Q. Effect of dielectric barrier discharge (DBD) plasma on the activity and structural changes of horseradish peroxidase. *Qual. Assur. Saf. Crops Foods* **2021**, *13*, 92–101. [[CrossRef](#)]
36. Wang, Y.; Ye, Z.; Li, J.; Zhang, Y.; Guo, Y.; Cheng, J.-H. Effects of dielectric barrier discharge cold plasma on the activity, structure and conformation of horseradish peroxidase (HRP) and on the activity of litchi peroxidase (POD). *LWT Food Sci. Technol.* **2021**, *141*, 111078. [[CrossRef](#)]
37. Han, Y.-X.; Cheng, J.-H.; Sun, D.-W. Changes in activity, structure and morphology of horseradish peroxidase induced by cold plasma. *Food Chem.* **2019**, *301*, 125240. [[CrossRef](#)]
38. Kiselyova, O.I.; Yaminsky, I.; Ivanov, Y.D.; Kanaeva, I.P.; Kuznetsov, V.Y.; Archakov, A.I. AFM study of membrane proteins, cytochrome P450 2B4, and NADPH-Cytochrome P450 reductase and their complex formation. *Arch. Biochem. Biophys.* **1999**, *371*, 1–7. [[CrossRef](#)]
39. Pleshakova, T.O.; Kaysheva, A.L.; Shumov, I.D.; Ziborov, V.S.; Bayzhanova, J.M.; Konev, V.A.; Uchaikin, V.F.; Archakov, A.I.; Ivanov, Y.D. Detection of hepatitis C virus core protein in serum using aptamer-functionalized AFM chips. *Micromachines* **2019**, *10*, 129. [[CrossRef](#)]
40. Sanders, S.A.; Bray, R.C.; Smith, A.T. pH-dependent properties of a mutant horseradish peroxidase isoenzyme C in which Arg38 has been replaced with lysine. *Eur. J. Biochem.* **1994**, *224*, 1029–1037. [[CrossRef](#)]
41. Ornelas-González, A.; Rito-Palomares, M.; González-González, M. TMB vs ABTS: Comparison of multi-enzyme based approaches for the colorimetric quantification of salivary glucose. *J. Chem. Technol. Biotechnol.* **2022**, *97*, 2720–2727. [[CrossRef](#)]
42. Enzymatic Assay of Peroxidase (EC 1.11.1.7) 2,20-Azino-Bis(3-Ethylbenzthiazoline-6-Sulfonic Acid) as a Substrate Sigma Prod. No. P-6782. Available online: <https://www.sigmaaldrich.com/RU/en/technical-documents/protocol/protein-biology/enzymeactivity-assays/enzymatic-assay-of-peroxidase-abts-as-substrate> (accessed on 18 February 2022).
43. Volume of a Pyramid or Cone. Available online: <https://www.khanacademy.org/math/geometry/hs-geo-solids/xff63fac4:hs-geo-cavalieri-s-principle/a/volume-of-a-pyramid-or-cone> (accessed on 17 November 2022).

44. Uniform Solid Tetrahedron, Pyramid and Cone. Available online: [https://phys.libretexts.org/Bookshelves/Classical_Mechanics/Classical_Mechanics_\(Tatum\)/01%3A_Centers_of_Mass/1.07%3A_Uniform_Solid_Tetrahedron%2C_Pyramid_and_Cone](https://phys.libretexts.org/Bookshelves/Classical_Mechanics/Classical_Mechanics_(Tatum)/01%3A_Centers_of_Mass/1.07%3A_Uniform_Solid_Tetrahedron%2C_Pyramid_and_Cone) (accessed on 18 February 2022).
45. Bunkin, A.F.; Nurmatov, A.A.; Pershin, S.M. Coherent four-photon spectroscopy of low-frequency molecular librations in a liquid. *Phys. Uspekhi* **2006**, *49*, 855–861. [[CrossRef](#)]
46. Pershin, S.M. A New Conception of the Action of EMF on Water/Aqueous Solutions, Taking into Account the Quantum Differences of the Ortho/Para of Spin Isomers of H₂O. Online Biophysical Blog. Available online: <http://www.biophys.ru/archive/sarov2013/proc-p17.pdf> (accessed on 3 October 2022).
47. Pershin, S.M.; Bunkin, A.F.; Golo, V.L. H₂O monomers in channels of icelike water structures. *J. Exp. Theor. Phys.* **2012**, *115*, 1008–1011. [[CrossRef](#)]
48. Artmann, G.M.; Kelemen, C.; Porst, D.; Büldt, G.; Chien, S. Temperature Transitions of Protein Properties in Human Red Blood Cells. *Biophys. J.* **1998**, *75*, 3179–3183. [[CrossRef](#)]
49. Fogarty, A.C.; Laage, D. Water Dynamics in Protein Hydration Shells: The Molecular Origins of the Dynamical Perturbation. *J. Phys. Chem. B* **2014**, *118*, 7715–7729. [[CrossRef](#)]
50. Laage, D.; Elsaesser, T.; Hynes, J.T. Water Dynamics in the Hydration Shells of Biomolecules. *Chem. Rev.* **2017**, *117*, 10694–10725. [[CrossRef](#)]
51. Ziborov, V.S.; Pleshakova, T.O.; Shumov, I.D.; Kozlov, A.F.; Valueva, A.A.; Ivanova, I.A.; Ershova, M.O.; Larionov, D.I.; Evdokimov, A.N.; Tatur, V.Y.; et al. The Impact of Fast-Rise-Time Electromagnetic Field and Pressure on the Aggregation of Peroxidase upon Its Adsorption onto Mica. *Appl. Sci.* **2021**, *11*, 11677. [[CrossRef](#)]